Proceedings of ASME-JSME-KSME Joint Fluids Engineering Conference 2011
AJK2011-FED
July 24-29, 2011, Hamamatsu, Shizuoka, JAPAN

AJK2011-19020

SWIMMING HYDRODYNAMICS AND MANEUVERABILITY IN C-START OF ZEBRAFISH LARVAE: AN INTEGRATED COMPUTATIONAL STUDY

Gen Li
Chiba University
Japan

Hao Liu
Chiba University
Japan

Ulrike K.Müller
California State University
USA

Johan L. van Leeuwen
Wageningen University
The Netherlands

ABSTRACT

Fishes often exhibit stable body undulating in body and caudal fin (BCF) mode during cyclic swimming, but can perform remarkable maneuverability with significantly different swimming modes in case of C-start. Aiming at unveiling the mechanisms of swimming hydrodynamics and maneuverability of C-start, we have developed an integrated computational framework to model a free-swimming larval zebrafish (*Danio rerio*) by coupling the equations of 3DoF (Degrees of Freedom) motion and Navier-Stokes (NS) equations. Unsteady hydrodynamics is resolved by integrating models of realistic fin-body morphology and body-undulatory kinematics with an *in-house* NS solver. The instantaneous forces and moments on the body provided by the NS-solutions serve as input for 3DoF equations of motion. In this study, with a specific focus on a C- start as well as a subsequent transient phase till the cyclic swimming phase, we construct a larval zebrafish model, which can mimics realistic body motions and deformations based on measurements. Validation of the simulation is discussed by comparing model predictions with experimental measurements, which indicates that the present integrated model is capable to accurately predict free-swimming dynamics and hydrodynamics. The model successfully simulated a swimming bout of C-start and cyclic swimming: a wake topology of double row vortex ring structures is observed behind the fish; and a strong jet is visible at the center of the vortex ring, pushing water backward as the fish accelerates.

Key words: computational fluid dynamics (CFD), C-start, free swimming, zebrafish

INTRODUCTION

Swimming by undulating body like other swimmers, the zebrafish larvae are living in an intermediate flow regime. Expressed by the Reynolds number ($Re=UL/\nu$, where U the swimming speed, L the body length of the fish, and ν the kinematic viscosity of the water), the ratio of inertial to viscous forces on a hatching fish such as zebrafish larvae is located in a range from Re=10 to 900. While the larger and faster swimmers experience mainly inertial force and the smaller and slower swimmers experience mainly viscous force, both inertial and viscous force play important roles when larvae is swimming [1,2].

Zebrafish larvae exhibit stable body undulating in body and caudal fin (BCF) mode during cyclic swimming, but can perform significantly different swimming modes in a fast-start swimming manoeuvres to avoid predators and to capture prey, which is distinguished into C-start and S-start [3]. A remarkable C-start phase includes a preparatory stroke, a propulsive stroke and a subsequent variable behavior [4]. During the preparatory stroke the body, represented by its midlines, adopts a C shape, then during the propulsive stroke the body straightens and the tail completes the first propulsive beat cycle and carries on swimming continuously. Some experimental researches have recorded the C-start motion of zebrafish larvae using high speed camera or two-dimensional digital particle image velocimetry (2D-DPIV) [5,6].

In order to unveil the mechanisms of swimming hydrodynamics and maneuverability of C-start in a computational avenue, we present an integrated computational framework to model a free-swimming larval zebrafish [7]. This integrated computational framework couples the equations of 3DoF (Degrees of Freedom) motion and Navier-Stokes (NS)

equations. Unsteady hydrodynamics is resolved by integrating models of realistic fin-body morphology and body-undulatory kinematics with an *in-house* NS solver. The instantaneous forces and moments on the body provided by the NS-solutions serve as input for 3DoF equations of motion.

In this study, a C-start and continuous swimming bout was reconstructed numerically. Special attention was paid to the jet flow and vorticity field during the C-start phase. Also, three-dimensional vortex pattern was discussed and during continuous swimming a wake topology of double row vortex ring structures were observed behind the fish. Here we not only present quantitative analysis of the kinematics and maneuverability, but also make comparison between experimental and computational result of the entire swimming bout.

INTEGRATED METHODS OF MODELING

Morphological Modeling

The object of this research is zebrafish (Danio rerio) larvae 5 days post-fertilization (d.p.f.), reared in the laboratory from wild-type parents. The average body length of 5 d.p.f. larvae is about 4.4mm.

A 3D nondimensionalized fish surface model was constructed and later applied to O-O type grid system generation work. In our previous study, the surface modeling work was accomplished by approximating each cross section along the body axis with ellipse, while in this study we adopted a more precise model, of which each cross section (45 cross sections in total, including head and tail tip) was setup individually according to the profile of real fish larvae.

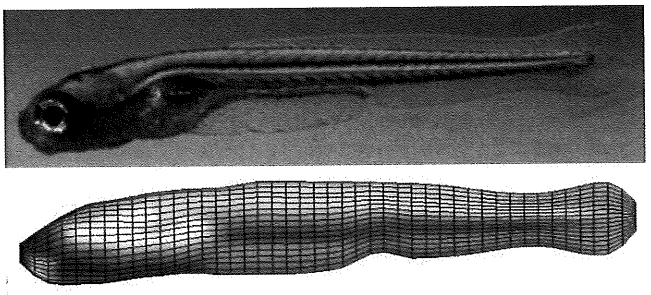

FIGURE 1. 5 D.P.F.REAL ZEBRAFISH (UPPER) AND MODEL (LOWER)

Deformation Modeling

Unlike in cyclic swimming phase, during a C-start the fish performs a C shape during the preparatory stroke to initiate a turn. The character of a C-start could not been expressed by a single sinusoidal function. On the other hand, in order to make the simulation comparable with real swimming course in experimental video, the deformation of fish model should be based on actual procedure, rather than a fixed theoretical function.

The motion of fish larvae was recorded by high speed camera, after that several tens of larvae body midline points were indicated manually according to fish's porfile in each frame. These raw midlines were interpolated and smoothed with cubic spline in space and time series. The parameters of the result midlines were then sent to the integrated solver as "Deformation Command".

As to the computational larvae model swimming in the virtual space, its midline followed the "Deformation Command", thus controlled the translation and rotation of model's cross sections, redeploying the whole grid system around fish model.

Grid System

In this study, a multi-blocked grid system was applied as demonstrated in Fig.2. A global H-H type (Cartesian-type, cyan mesh in Fig.2) grid was set as a "water tank". An O-O type grid (violet mesh in Fig.2) enveloping the larvae's body surface was deployed inside the global H-H grid. The dimension of the global grid was 55×111×75 (length×height×width), large enough to cover the path of larvae's motion; the body-fitted grid was 33×45×20, respectively in circumferential, axial and radial direction.

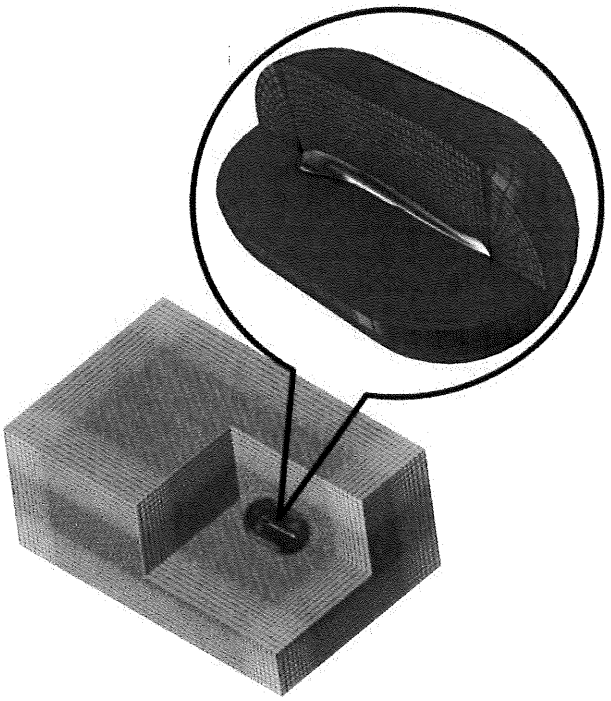

FIGURE 2. COMPUTATIONAL GRID SYSTEM

Computational Fluid Dynamic (CFD) Modeling

An *in-house* CFD (computational fluid dynamic) model based on the multi-blocked, overset-grid, dynamic moving-boundary, fortified solutions to the Navier-Stokes equations was employed, of which the governing equations are the incompressible, unsteady Navier-Stokes equations, expressed in strong conservative form for momentum and mass.

Of the multi-blocked grid system, both grid blocks possess specific boundary conditions. On the body surface of the O-O type grid around the fish, the no-slip condition is used for the velocity components whereas the dynamic effect due to the body's acceleration/deceleration is taken into account for pressures.

$$(u, v, w) = (u_{body}, v_{body}, w_{body})$$
$$\partial p / \partial n = -a_0 \cdot n \quad (1)$$

where the velocity (u_{body}, v_{body}, w_{body}) and the acceleration (a_0) on the solid wall are evaluated and updated using the renewed grids on the surface at each time step.

In global H-H grid, upstream is set as $(u, v, w, p) = (0, 0, 0, 0)$, while at downstream and side boundaries zero-gradient condition is taken for both velocity and pressure, i.e., $\partial(u, v, w, p)/\partial \boldsymbol{n} = 0$, where $\boldsymbol{n}$ is the unit outward normal vector at the outside boundary.

In the low Reynolds number regime, this CFD model has been proofed capable to accurately compute unsteady biological fluid dynamics. More description and validation can be found in [8-10].

Computational Swimming Dynamic (CSD) Modeling

The dynamic model is constructed upon the assumption that: fish such as zebrafish larvae carry out movement in the BCF (Body and Caudal Fin propulsion) mode and the fish's body deformation solely happens in horizontal plane. Pitch-and roll motions are mainly due to the geometric asymmetry between superior and inferior parts (the yolk-sac, for example, is one of the main geometric asymmetry factors). The pectoral fins, excluded in this study, are expected to sustain the body attitude against roll and pitch. Thus among the three rotational freedoms yaw-motion is merely put into consideration while pitch-and roll-motions are neglected.

A nonlinear single deform-body dynamic model can be constructed based on the Newton-Euler equations of 3 DoF (degree of freedom) motion as a set of four coupled nonlinear ordinary differential equations, such as:

$$\boldsymbol{M}\frac{d\boldsymbol{V}_{CG}}{dt} = \boldsymbol{F}$$
$$\boldsymbol{I}\frac{d\omega}{dt} = \boldsymbol{N} \quad (2)$$

where $\boldsymbol{F}$ is the fluid force acting on the body surface, and $\boldsymbol{V}_{CG}$=(U_{CG}, V_{CG}, W_{CG}) is the translational velocity of the center of mass of the body, ω its global angular velocity about the y-axis, M the total mass, and I the moment of inertia and N the hydrodynamic moment about the y-axis. The three force components (F_x, F_y, F_z) exerted on the body surface in the global system are evaluated by a summation of inviscid and viscous fluxes over the body surface:

$$\mathrm{F} = \begin{bmatrix} F_x \\ F_y \\ F_z \end{bmatrix} = -\sum_{i}^{body} \left(Flux_{inviscid} + Flux_{viscous} \right) \quad (3)$$

The hydrodynamic moment $\boldsymbol{N}$ is calculated as the sum of the cross product of each force and the positional vector at each cell center on the body surface, such that:

$$\boldsymbol{N} = \sum_{i}^{body} \left(\boldsymbol{r}_i \times \boldsymbol{F}_i \right) \quad (4)$$

where $\boldsymbol{r}_i$ denotes the positional vector of the i-th cell center on the body surface, and $\boldsymbol{F}_i$ is the hydrodynamic force vector at the i-th cell center. Body mass M is assumed constant but the yawing moment of inertia I varies with time and is updated at each time step.

By coupling with the NS solver, we directly solve the nonlinear equations of 3DoF motion numerically with a second-order Runge-Kutta method to get the time variations of the four velocity variables (U_{CG}, V_{CG}, W_{CG}, ω). The three hydrodynamic force components F_x, F_y, F_z and moment N on the right hand side (RHS) of the equation (2) are given by equations (3) and (4) based on the NS solutions.

Furthermore, in the occasion of fish body grid's deformation update, mass of the body is approximately considered concentrated into fish's central line. Through solve the interaction among elements in this linkage mechanism, approximate inertial force effect thus included in the CSD system.

RESULTS AND DISCUSSION

Simulation Target: A Swimming Bout Consisting of a C-Start and Cyclic Phase

The object of experiment is wild type Zebrafish danio 5 days after fertilization with a body length of 4.38 mm

As showed in Fig.3, in the water tank the zebrafish larva was artificially stimulated on its tail fin tip by thin stick (Fig.3 A). Fish then performed a C-start from rest with an initially straight body, curving its body into a C-shape, combined with a small turn without conspicuous forward movement (Fig.3B). After the preparatory stroke (tail beat 1) fish carried out a powerful propulsive stroke (tail beat 1), accelerated dramatically (Fig.3C) and continued to swim steadily until it leaves the field of view. The pectoral fins remained abducted throughout the entire sequence.

Consisting of 46 frames, recorded at 1000 Hz, the midline splines of fish larvae ware demonstrated in time series (Fig.3D). Midlines at the end of each stroke are bold, in addition, trajectories of head and tail tips are also marked respectively in green and red.

The mean swimming speed was 40.73 [BL/s], mean tail

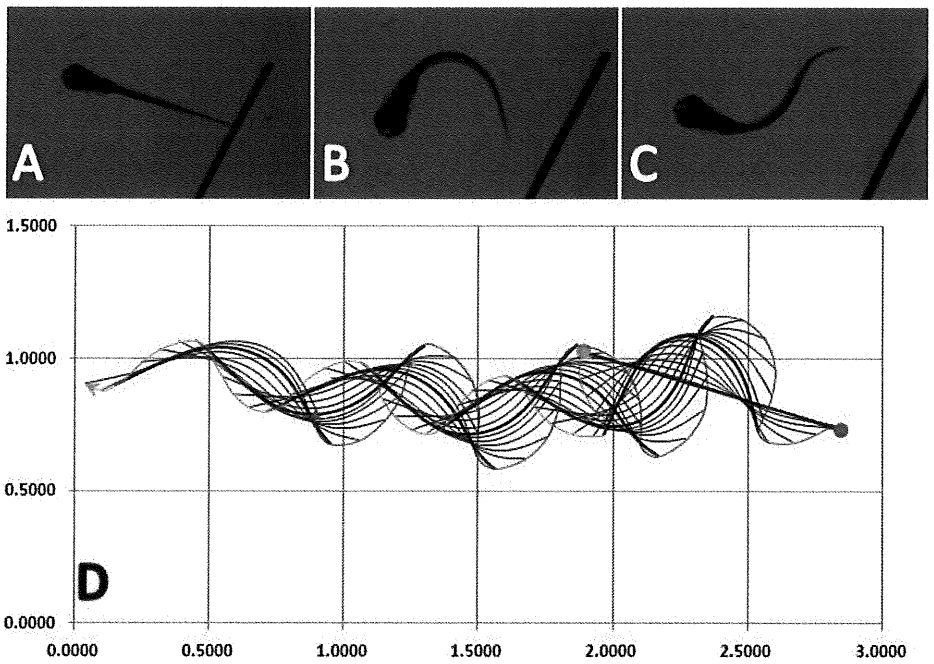

FIGURE 3. FISH PROFILES OF STEADY (A), PERPARATORY STROKE (B), PORPULSIVE STROKE (C) AND MIDLINE SPLINE SERIES (D)

beat frequency f=93.75 Hz, mean body wave length 1.08 BL, thereby the computational simulation was setup at a Reynolds Number of 900.

Two-Dimensional Velocity Field Simulation of C-start

The computational result of velocity field in horizontal plane across the middle height of the fish body, from the beginning of preparatory stroke to the end of the first propulsive stroke, is demonstrates in Fig.4: the preparatory stroke produced two main jet flow, both initially lateral. One of the two followed the swing of the tail fin to the left while the other moved towards the concave part of the C-Shaped body in the opposite direction of the tail (Fig.4 2-4ms). At the end of preparatory stroke jet flow at the tail tended to move forward slightly, decelerating and yawing the fish consequentially (Fig.4 7ms). After that, the first propulsive stroke produced a powerful jet backward (Fig.4 9-13ms), in the meanwhile another propulsive flow was forming (Fig.4 15ms).

Two-Dimensional Vorticity Field Simulation of C-start

The two-dimensional vorticity field is demonstrated as Fig.5. At the beginning preparatory stroke, four main vortex zones appeared along the fish body. During the preparatory and propulsive stroke, the evolution of those vorticity was closely related to that of the jet flows lying between each two adjacent vorticity. By the end of the preparatory stroke, the first vortex pair (vortex 1 & 2 in Fig.5 7-9ms) shed, vortex 2 then appeared to separate into two sub-vorticity (vortex 2L & 2R in Fig.5 11-15ms). The sub-vortex on the right, along with vortex 3, composed another vortex pair shed when the first propulsive stroke finished (vortex 2R & 3 in Fig.5 11-15ms).

After the C-start, vortex pairs kept being generated during continuous swimming (cyclic swimming). All of these vortex pairs, in 3-dimensional view, were cross sections of vortex rings.

Three-Dimensional Vorticity Field Simulation

Figure.6 shows 3-dimensional iso-vorticity surface (vorticity = 1.5) at different time, the surface is set semi-transparent for better view of the vortex structure and colored according to local flow speed.

The preparatory stroke generated vertex ring 1(VR.1), which moved and weakened together with the preparatory jet flow (Fig.6 A). Later the propulsive stroke produced another powerful jet flow and vertex ring 2 (VR.2) around the jet (Fig.6 B), and went on generating new vorticity during cyclic swimming while former vertex rings were fading away(Fig.6 C). During entire swimming bout vortex rings apparently formed a double row array (Fig.6 D).

As to the structure of the vortex rings, strong jet flow could be detected in center of each vortex ring. Two neighborhood vortex rings linked when newly born, and isolated as they moving separately and weakening.

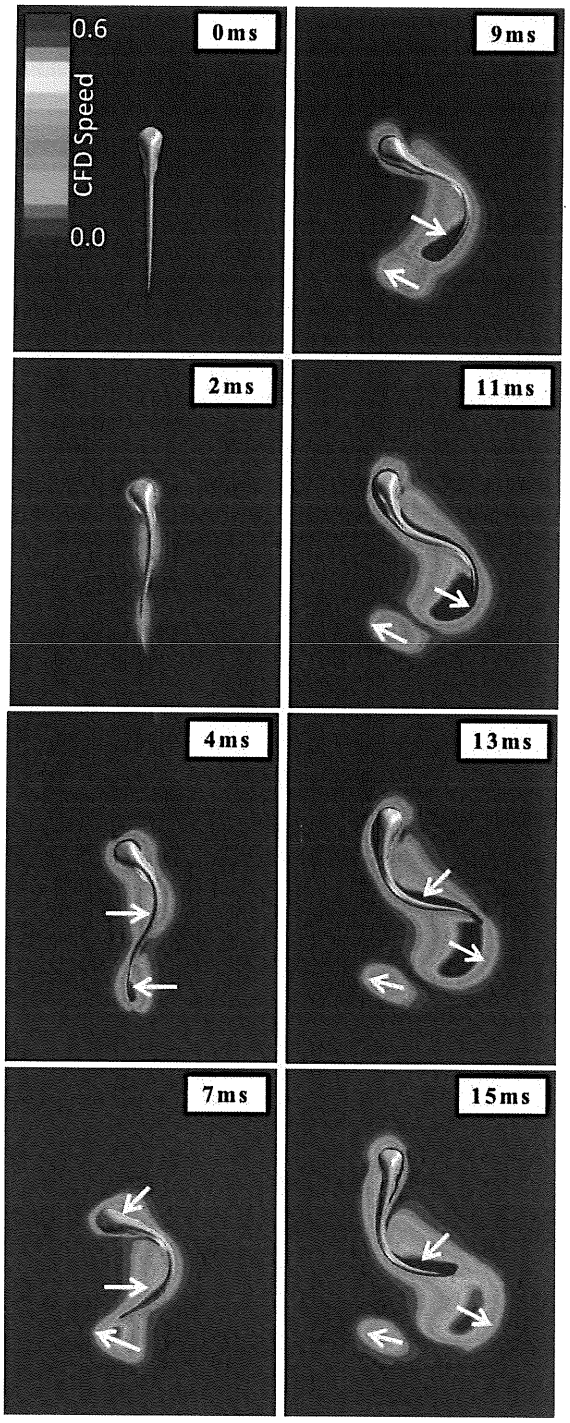

FIGURE 4. 2D VELOCITY FIELD SIMULATION OF C-START

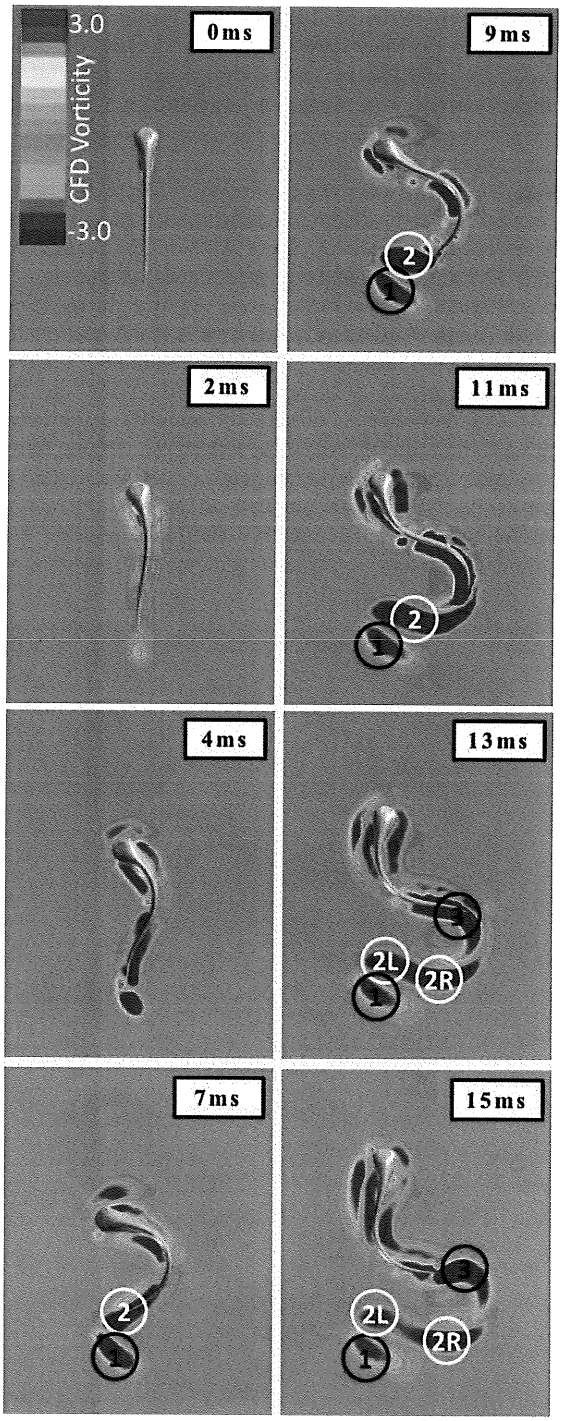

FIGURE 5. 2D VORTICITY FIELD SIMULATION OF C-START

Kinematics Simulation of C-Start and Cyclic Swim

According to the kinematics result (Fig.7), the fish, when carrying out the preparatory stroke (tail beat1), took slight displacement laterally, but rotated dramatically. The first propulsive stroke (tail beat2) played the most important role in fish's acceleration and stops the spin.

During the cyclic swimming after the C-start, the fish's velocity tended to steady, displacement increased smoothly, and head angle oscillated, all of these kinematics parameters represented regularly undulated curves in sinusoidal pattern.

The computational velocity was slightly lower than experimental result. A question raised here is that, traditionally the condition of the fluid in a straight swimming bout is expressed by Reynolds Number calculated based on the velocity of CG, however in this complicated case the larva began with a C-start, during which the fish struck with no effort spared but made slight displacement. Hence Reynolds Number used here is possibly underestimated. Also, the interaction among stimulatory stick, fish and flow field also affected and brought more error. The velocity error accumulated, resulting in a displacement error rate of approximately 9% by the end of tail beat 7, as well as error in swimming direction.

The computational trajectory of fish's entire swimming bout is transformed into coordinates of source video data (Fig.8), and the body profiles at the end of tail beat 1, 4, 7 are picked out and compared to experimental profiles.

CONCLUSION

In this study an integrated computational framework is developed to model a free-swimming larval zebrafish by coupling the equations of 3DoF (Degrees of Freedom) motion and Navier-Stokes (NS) equations. We then carried out a systematic computational study to simulate a specific swimming bout consisting of a C-start and cyclic phase. The velocity and vorticity field of the C-start were obtained, as well as the computational kinematics result of hydrodynamics and maneuverability of the entire swimming bout. The computational kinematics result is basically correct while further work is expected to examine the prediction.

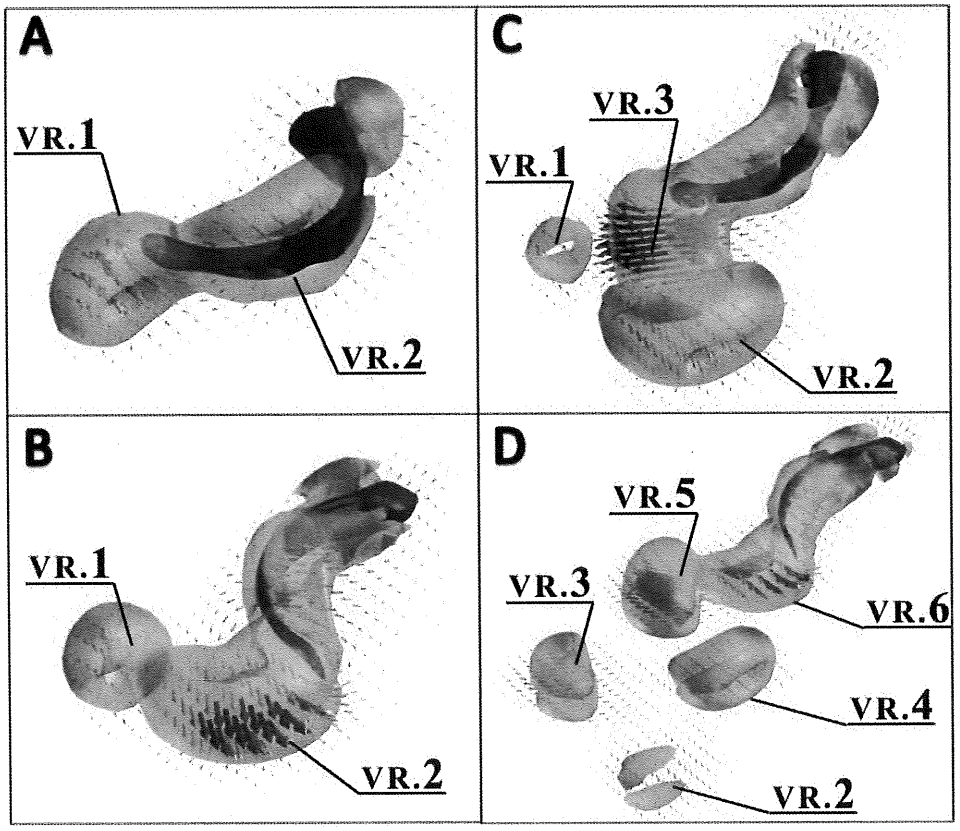

FIGURE 6. 3-DIMENSIONAL ISO-VORTICITY SURFACE (VORTICITY=1.5) AT DIFFERENT TIME

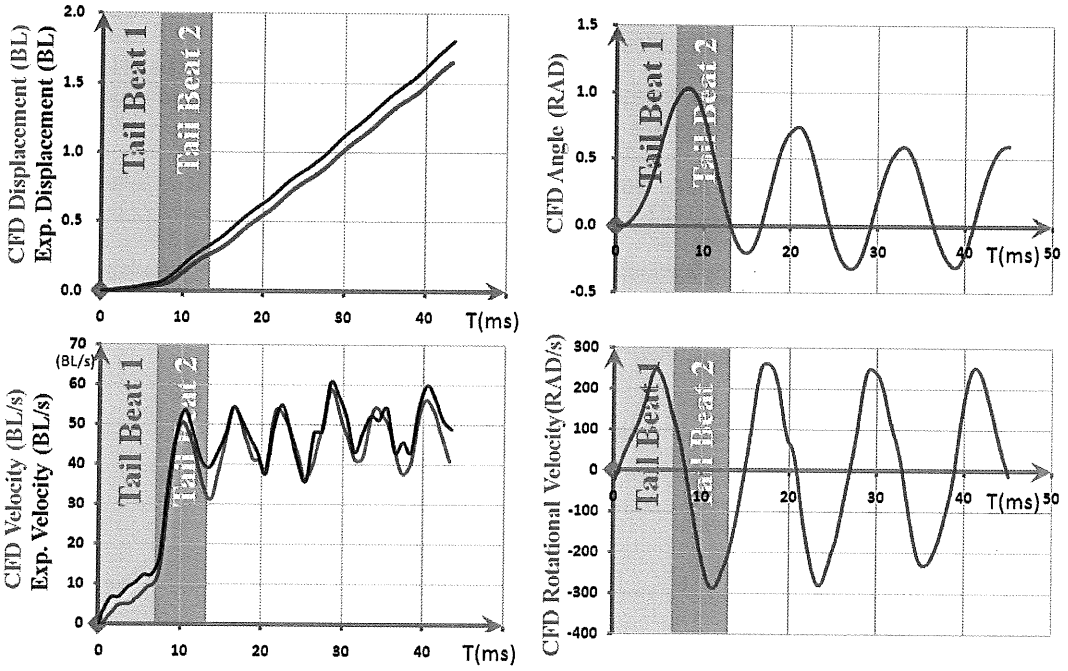

FIGURE 7. COMPUTATIONAL KINEMATICS RESULT OF ENTIRE SWIMMING BOUT

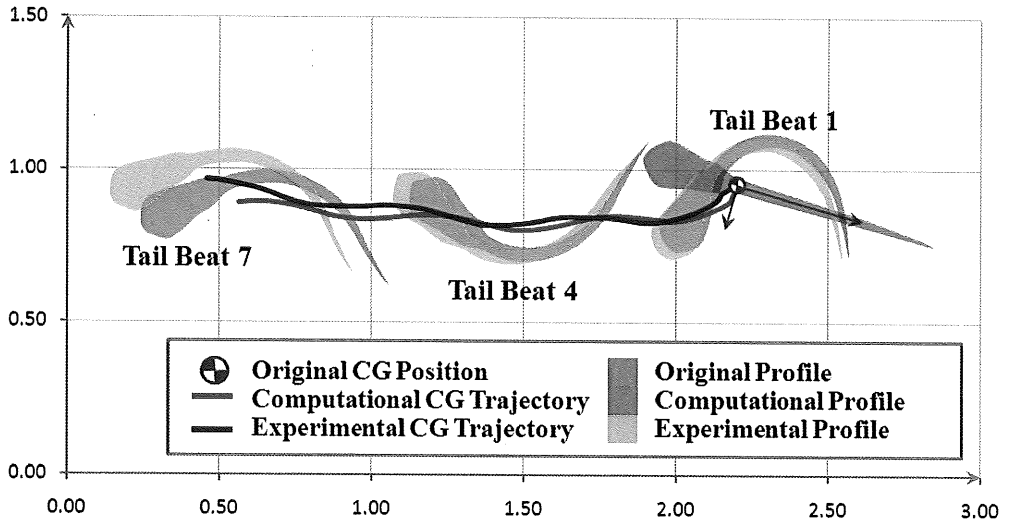

FIGURE 8. ENTIRE COMPUTATIONAL TROJECTORY AND CONTRAST OF PROFILES

ACKNOWLEDGMENTS

This work was partly supported by a PRESTO-JST program, and the Grant-in-Aid for Scientific Research of No. 18656056 and No. 18100002, JSPS, Japan. UKM was funded by NWO-ALW grant 814.02.006 and a JSPS fellowship. HL was also funded by a CKSP fellowship.

REFERENCES

[1] Fuiman, L.A. and Batty, R.S. (1997). What a drag it is getting cold: partitioning the physical and physiological effects of temperature on fish swimming. *J. Exp. Biol.* 200.1745-1755.

[2] McHenry, M. J. and Lauder., G. V. (2005). The mechanical scaling of coasting in zebrafish (Danio rerio), *J. Exp. Biol.* 205,2289-2301.
[3] Spierts, I. L. Y. and van Leeuwen, J. L. (1999). Kinematics and muscledynamics of C- and S-starts of carp (Cyprinus carpio L.). *J. Exp. Biol.* 202,393-406.
[4] Webb, P. W. (1978b). Fast-start performance and body form in seven species of teleost fish. *J. Exp. Biol.* 74, 211–226.
[5] Müller, U. K. and Leeuwen, J. L. (2004). Swimming of larval zebrafish: ontogeny of body waves and implications for locomotory development. *J. Exp. Biol.* 207, 853-868.
[6] Müller, U. K., van den Boogaart, J. G. M. and van Leeuwen, J. L. (2008). Research article Flow patterns of larval fish: undulatory swimming in the intermediate flow regime. *J. Exp. Biol.* 211, 196-205.
[7] Katumata, Y., Müller, U. K. and Liu, H. (2009). Computation of self-propelled swimming in larva fishes. *Journal of Biomechanical Science and Engineering*, 4(1), 54-66.
[8] Liu, H. and Kawachi, K. (1999). A numerical study of undulatory swimming. *J. Comput. Phys.* 155, 223.
[9] Liu, H. (2005). Simulation-based biological fluid dynamics in animal locomotion. *Appl. Mech. Rev.* 58, 269-282.
[10] Liu, H. (2009). Integrated modeling of insect flight: From morphology, kinematics to aerodynamics. *J. Comput. Phys.* 228, 439-459.